# Black-eye patterns: A representation of three-dimensional symmetries in thin domains

M. Gabriela M. Gomes*
*Centro de Matemática Aplicada, Universidade do Porto, Rua das Taipas 135, 4050 Porto, Portugal*
(Received 2 November 1998)

What is believed to be the first experimental evidence for Turing patterns was observed in the CIMA reaction by De Kepper and colleagues. Ouyang and Swinney performed further experiments in a ''thin'' layer of gel. Patterns observed at onset were basically two-dimensional. However, beyond onset a structure that does not typically occur in two-dimensional domains was observed—the black-eye pattern. In this paper we use the full three-dimensionality of the patterned layer to find a setting where black-eye patterns naturally occur. We propose that black-eye patterns have the symmetry of a body-centered-cubic lattice.
[S1063-651X(99)06910-X]

PACS number(s): 47.54.+r, 02.20.Qs, 47.20.Ky

## I. INTRODUCTION

Pattern formation in thin domains is often formulated as a planar problem. Examples include models for animal coat pattern formation [1], application of symmetric bifurcation theory [2] to pattern formation in Rayleigh-Bénard convection [3], the Newell-Whitehead-Segel equation [4], and its Euclidean invariant version [5,6]. These two-dimensional approaches are often satisfactory. However, there is evidence of natural and experimental patterns whose highly developed structure is surprising in purely two-dimensional systems.

The formation of spatial patterns in reaction-diffusion systems, predicted by Turing [7], was first observed experimentally by De Kepper and colleagues [8], working with the chlorite-iodide-malonic acid (CIMA) reaction in an open thin strip gel reactor. Ouyang and Swinney [9] performed a series of experiments on the same reaction, occurring in a thin disc of gel contained between two continuously fed well-stirred reactors. By varying the control parameter, hexagonal or striped patterns emerged spontaneously from the uniform state. Beyond the onset of Turing patterns, the authors observe transitions to more complex stationary patterns, including rhombic structures, zigzags, and black eyes. The Euclidean invariant envelope equation developed by Gunaratne *et al.* [5,6] reproduces many of the experimental observations. The theory is developed under the assumption that, due to the thinness of the domain, the selected patterns are basically two-dimensional.

A black-eye pattern, reproduced from Ref. [6], is shown in Fig. 1. The Fourier transform reported in the same reference shows that this structure consists of the superposition of two hexagonal arrays of spots with different wavelengths in the ratio $\sqrt{3}$. Linear superpositions of such modes are not expected in purely two-dimensional systems. Gunaratne *et al.* [5,6] propose that since these patterns occur away from onset, they can be justified as spatial harmonics generated by *nonlinear* interactions of the basic modes responsible for the hexagonal pattern observed at onset. However, the authors point out that in the experiments the harmonics were not detected until well beyond the onset of hexagons, while from the analysis one would expect the amplitudes of the harmonics to grow continuously beyond the primary instability. In Sec. VI of Ref. [6], the authors express their concern about this discrepancy, and suggest that it could be due to insufficient sensitivity in the experiments, or perhaps the secondary modes should not be ''slaved'' to the primary modes as their theory had assumed.

To our knowledge, black-eye patterns have not been reported in other prototype pattern forming systems, such as convection. Pattern formation is considered a very universal phenomenon which is, to a large degree, determined by symmetry considerations. The two-dimensional symmetry description given in Ref. [6] places the CIMA reaction in the same symmetry class, for example, as Bénard-Marangoni convection or Rayleigh-Bénard convection in non-Boussinesq fluids. This argument leads very naturally to the question: Why have black-eye patterns not been reported in experimental studies of pattern formation in convection? A simple but subtle answer is that the reaction-diffusion mechanism has an intrinsic isotropy (which is not present in

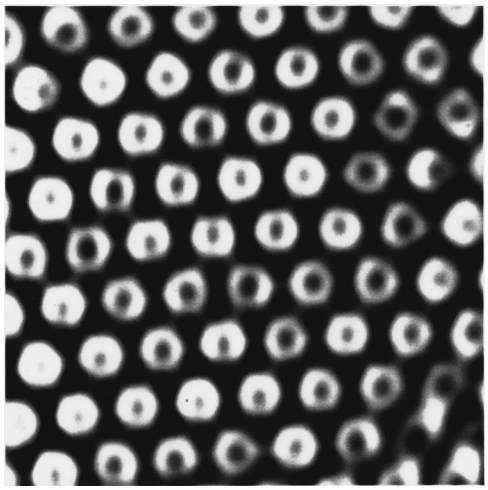

FIG. 1. Black-eye pattern observed experimentally by Ouyang and Swinney. (Reprinted with permission from Ref. [6].)

*Present address: Ecology and Epidemiology Group, Department of Biological Sciences, University of Warwick, Coventry CV4 7AL, United Kingdom. Electronic address: mgmg@maths.warwick.ac.uk

 

convection) that introduces three-dimensional symmetries into the problem.

Independent studies, based on the inclusion of general symmetry considerations in the Landau theory of nonequilibrium phase transitions, have shown strong evidence that body-centered-cubic (bcc) structures are the most favored crystal structures near the melting line [10]. By analogy with this work, it was shown that bcc structures are the most stable Turing patterns in a three-dimensional space [11]. Numerical simulations of the Brusselator model of the Turing instability [12] confirmed the theoretically predicted three-dimensional patterns. Such patterns, which include bcc, were obtained for isotropic systems, and also in the presence of gradients such as those due to feeding fluxes. A more detailed study of pattern selection in three-dimensional Turing systems was recently completed [13] by center manifold reduction of two reaction-diffusion models—the Brusselator and the more realistic Lengyel-Epstein model for the CIMA reaction.

The black-eye pattern observed in the CIMA reaction by Ouyang and Swinney forms a layer whose thickness is comparable to the pattern wavelength. Naively, in a system whose aspect ratio (size of domain to wavelength) is not very large, one would not expect symmetries that do not leave the domain invariant. However, it is not unusual to find unexpected conjugacies and unexpected highly developed patterns in small aspect ratio systems. The presence of unexpected Euclidean symmetry effects was noticed and carefully investigated by several researchers during the last 20 years (see Ref. [14] for a review including many references). Such spatial symmetries are known as *hidden symmetries*.

It was also independently established by Winfree [15] that certain wave patterns observed in thin layers of liquid malonic acid reagent are best interpreted as three-dimensional structures seen in projection.

This paper uses three-dimensional Euclidean symmetries to propose a theory for the occurrence of black eyes, in alternative to that proposed in Ref. [6]. The thin domain is considered as a slice of a fully three-dimensional problem whose symmetry is described by a lattice in three dimensions. The lattice underlines the construction of spatially periodic functions (planforms) in $\mathbb{R}^3$. The corresponding sliced planforms have now a three-dimensional characterization and different planforms may have different structures in the thin direction. As a result, we find symmetries that are not expected in planar systems. In particular, black-eye patterns are expected as a slice of a bcc planform, which is a favorite structure in three dimensions. In contrast with the theory proposed in Ref. [6], we propose a scenario where the black-eye pattern occurs as a *linear* mode. This distinction may have important consequences in future directions for pattern formation studies.

The remainder of this paper is organized as follows. Section II begins with the formulation of a generic $E(3)$-invariant bifurcation problem, and its restriction to spatial periodicity. This is followed by the demonstration of how the black-eye pattern is obtained as a slice of the bcc pattern. Comparison with the experimental pattern obtained by Ouyang and Swinney is made at the end of the section. In Sec. III, we discuss at length further issues related to the application of the theory to the experiments, and propose further investigations. We stress the importance of investigations towards better resolving the thickness of the ''patterned layer'' and its ''boundaries,'' and understanding how the pattern selection varies with the thickness of the gel layer. Finally, our conclusions are summarized in Sec. IV.

## II. THE BIFURCATION PROBLEM

In Secs. II A and II B we briefly describe how group theoretical techniques developed by Golubitsky *et al.* [2] are used to construct a general scenario for the onset of spatially periodic patterns (planforms) in three dimensions. The two sections (which are included here for completeness) refer the interested readers to related work. However, readers who wish to skip the general abstract formulation can go straight to Secs. II C and II D, where we consider the particular case of body-centered-cubic (bcc) structures. There we show that black-eye patterns can occur as a linear instability in a thin layer if the full three-dimensionality of the patterned layer is taken into account.

### A. The $E(3)$-invariant problem

Following Dionne and Golubitsky [16,17], let $\mathcal{P}$ denote an elliptic operator (e.g., reaction diffusion) between function spaces $\mathcal{X}$ and $\mathcal{Y}$. We are interested in steady solutions of the partial differential equation

$$u_t + \mathcal{P}(u,\mu) = 0, \tag{2.1}$$

where $\mu \in \mathbb{R}$ is a bifurcation parameter and, for simplicity, where $u$: $\mathbb{R}^3 \to \mathbb{R}$ is restricted to being a scalar function (often when considering bifurcations the general situation of $u$: $\mathbb{R}^3 \to \mathbb{R}^m$ reduces to this case). We assume that $\mathcal{P}$ is equivariant under an action of the Euclidean group $E(3)$ consisting of a semidirect sum of the group of rotations and reflections, $O(3)$, with the group of translations, $\mathbb{R}^3$. The action of $\gamma \in E(3)$ on $u$ is induced by the action on $\mathbb{R}^3$ as

$$(\gamma u)(x) = u(\gamma^{-1}x). \tag{2.2}$$

Assume that there is a trivial solution $u=0$, which undergoes a generic steady-state bifurcation when $\mu$ is varied across a critical value $\mu_c$. More formally, the linearization, $L_{\mu_c} = (d\mathcal{P})_{(0,\mu_c)}$, has a nontrivial kernel and, as the parameter $\mu$ crosses the critical value $\mu_0$, the eigenvalues that go through zero do so with nonzero speed [this is to say that if $\sigma(\mu)$ is an eigenvalue that varies with the parameter $\mu$ such that $\sigma(\mu_0)=0$, then $(d\sigma/d\mu)(\mu_0) \neq 0$]. Without further assumptions, a genericity condition states that the kernel of the linearized operator above is an irreducible representation of the group $E(3)$.

### B. Restriction to a spatially periodic problem

Dionne and Golubitsky [16,17] restrict their analysis to spatially periodic steady solutions and classifying the possible planforms. To find spatially periodic solutions, the authors fix a lattice $\mathcal{L}$ in $\mathbb{R}^3$ and demand that

$$u(x+l) = u(x) \tag{2.3}$$

for all $l \in \mathcal{L}$. Functions satisfying Eq. (2.3) are called $\mathcal{L}$ periodic. Denoting by $\mathcal{X}_\mathcal{L}$ and $\mathcal{Y}_\mathcal{L}$ the spaces of $\mathcal{L}$-periodic functions in $\mathcal{X}$ and $\mathcal{Y}$, respectively, the Euclidean equivariance of $\mathcal{P}$ implies that

$$\mathcal{P}: \mathcal{X}_\mathcal{L} \times \mathbb{R} \to \mathcal{Y}_\mathcal{L}. \tag{2.4}$$

The group $E(3)$ acts on $\mathcal{L}$-periodic mappings as the semidirect sum, $\Gamma = H \dot{+} T^3$, where $H$ is the group of rotations and reflections that leave the lattice $\mathcal{L}$ invariant (holohedry as in Ref. [18], or point operation as in Ref. [19]), and the three torus, $T^3 = \mathbb{R}^3/\mathcal{L}$, is the effective action of translations. The operator $\mathcal{P}$ in Eq. (2.4) is $\Gamma$ equivariant, and the kernel of the linearization, $L_{\mu_c}$, in the space of $\mathcal{L}$-periodic functions is generically an irreducible representation of the same group [2].

Now we say that $\boldsymbol{m} = (m_x, m_y, m_z)$ is a wave vector if and only if the complex-valued plane wave

$$w_{\boldsymbol{m}}(\boldsymbol{x}) = e^{2\pi i(\boldsymbol{m}\cdot\boldsymbol{x})} \tag{2.5}$$

is $\mathcal{L}$ periodic. The corresponding wave number is defined as $m_c = |\boldsymbol{m}|$. It is natural to define the dual lattice, $\mathcal{L}^*$, as the set of all $\boldsymbol{m} \in \mathbb{R}^3$ such that the associated plane wave, $w_{\boldsymbol{m}}$, is $\mathcal{L}$ periodic, or equivalently,

$$\mathcal{L}^* = \{\boldsymbol{m} \in \mathbb{R}^3 : (\boldsymbol{m}\cdot l) \in \mathbb{Z} \text{ for all } l \in \mathcal{L}\}. \tag{2.6}$$

(In the terminology of Ref. [19], $\mathcal{L}^*$ corresponds to the reciprocal lattice.)

For the given lattice $\mathcal{L}$ we assume that there exists a critical parameter value $\mu_c$ and a wave vector $\boldsymbol{m}$ such that the real-valued function

$$v_{\boldsymbol{m}}(\boldsymbol{x}) = z_{\boldsymbol{m}} w_{\boldsymbol{m}}(x) + \overline{z_{\boldsymbol{m}}} w_{-\boldsymbol{m}}(x) \tag{2.7}$$

is an eigenfunction for the linearization $L_{\mu_c}$, where $z_{\boldsymbol{m}}$ and $\overline{z_{\boldsymbol{m}}}$ are the complex amplitudes of the plane waves $w_{\boldsymbol{m}}$ and $w_{-\boldsymbol{m}}$, respectively. The $H$ equivariance of $L_{\mu_c}$ implies that if $v_{\boldsymbol{m}}$ is an eigenfunction, then so is $v_{\boldsymbol{m}'}$, for every $\boldsymbol{m}' \in \mathcal{L}^*$ having the same absolute value as $\boldsymbol{m}$. Consequently, a typical eigenfunction is a real-valued function of the form

$$u(\boldsymbol{x}) = \sum_{|\boldsymbol{m}| = m_c} z_{\boldsymbol{m}} e^{2\pi i(\boldsymbol{m}\cdot\boldsymbol{x})}, \tag{2.8}$$

where the wave vectors $\boldsymbol{m}$ are elements of $\mathcal{L}^*$ that have wave number $m_c$, and the $z_{\boldsymbol{m}}$ satisfy the reality condition $z_{-\boldsymbol{m}} = \overline{z_{\boldsymbol{m}}}$.

A complete classification of steady triply periodic bifurcations is a large problem, and is usually restricted to subclasses that exhibit particular features. Dionne [17] lists the holohedries, $H$, of the 14 Bravais lattices in three dimensions (see also Refs. [18,19]), and classifies the expected planforms with maximal symmetry in $H \dot{+} T^3$-invariant bifurcation problems. Callahan and Knobloch [20] perform a bifurcation analysis restricted to the simple representations with cubic symmetry, $H = \mathbb{O} \oplus Z_2^c$, where $\mathbb{O}$ is the octahedral group and $Z_2^c$ represents the center reflection. Gomes and Stewart [21] consider representations of higher dimension, but restrict the bifurcation analysis to the subspace of eigenfunctions that satisfy Neumann boundary conditions in a cubic domain.

### C. Black-eye pattern in a slice of bcc

In this section, we restrict attention to the bcc lattice. Special interest will be devoted to one of the maximal planforms predicted by Dionne [17]—the bcc pattern. We consider $\mathcal{L}$ as the bcc lattice generated by

$$l_1 = \left(\frac{1}{\sqrt{2}}, 0, \frac{1}{\sqrt{2}}\right), \quad l_2 = \left(\frac{1}{\sqrt{2}}, -\frac{1}{\sqrt{2}}, 0\right),$$

$$l_3 = \left(\frac{1}{2\sqrt{2}}, -\frac{1}{2\sqrt{2}}, \frac{1}{2\sqrt{2}}\right). \tag{2.9}$$

The dual lattice, $\mathcal{L}^*$, is generated by the vectors

$$\boldsymbol{m}_1 = (\sqrt{2}, 0, \sqrt{2}), \quad \boldsymbol{m}_2 = (\sqrt{2}, -\sqrt{2}, 0),$$

$$\boldsymbol{m}_3 = (0, -\sqrt{2}, \sqrt{2}). \tag{2.10}$$

Other vectors in $\mathcal{L}^*$ with the same length, $m_c = 2$, are obtained by changing the sign of individual components of $\boldsymbol{m}_1, \boldsymbol{m}_2, \boldsymbol{m}_3$. These operations lead to a fundamental representation with dimension 12. Substituting these wave vectors in the eigenfunction $u$ as in Eq. (2.8) and making the amplitudes $z_{\boldsymbol{m}}$ all real and equal, we generate a typical bcc pattern, as shown in Fig. 2. This is one of the expected planforms in bifurcation problems with bcc symmetry. Interestingly, and also shown in the figure, a black-eye pattern can be observed in the section $z = x + y$.

The relation between bcc and black-eye patterns becomes clear by applying the orthonormal change of coordinates

$$A = \begin{pmatrix} \frac{1}{\sqrt{2}} & \frac{-1}{\sqrt{2}} & 0 \\ \frac{1}{\sqrt{6}} & \frac{1}{\sqrt{6}} & \frac{2}{\sqrt{6}} \\ \frac{1}{\sqrt{3}} & \frac{1}{\sqrt{3}} & \frac{-1}{\sqrt{3}} \end{pmatrix}. \tag{2.11}$$

By transforming $\alpha_j = A l_j$, we obtain the generators of the body-centered-cubic lattice in the form

$$\alpha_1 = \left(\frac{1}{2}, \frac{\sqrt{3}}{2}, 0\right), \quad \alpha_2 = (1,0,0), \quad \alpha_3 = \left(\frac{1}{2}, \frac{\sqrt{3}}{6}, -\frac{1}{2\sqrt{6}}\right). \tag{2.12}$$

By applying the change of coordinates $\boldsymbol{X} = A\boldsymbol{x}$, the eigenfunction $u$ is rewritten as

$$u(\boldsymbol{X}) = \sum_{|\boldsymbol{k}| = k_c} z_{\boldsymbol{k}} e^{2\pi i(\boldsymbol{k}\cdot\boldsymbol{X})} + \overline{z_{\boldsymbol{k}}} e^{-2\pi i(\boldsymbol{k}\cdot\boldsymbol{X})}, \tag{2.13}$$

where $\boldsymbol{k} = \boldsymbol{m}A^{-1}$. Note that $k_c = m_c$ due to the orthonormality of the change of coordinates $A$. In the new coordinates, the generators $\boldsymbol{m}_1, \boldsymbol{m}_2, \boldsymbol{m}_3$ of the dual lattice $\mathcal{L}^*$ are

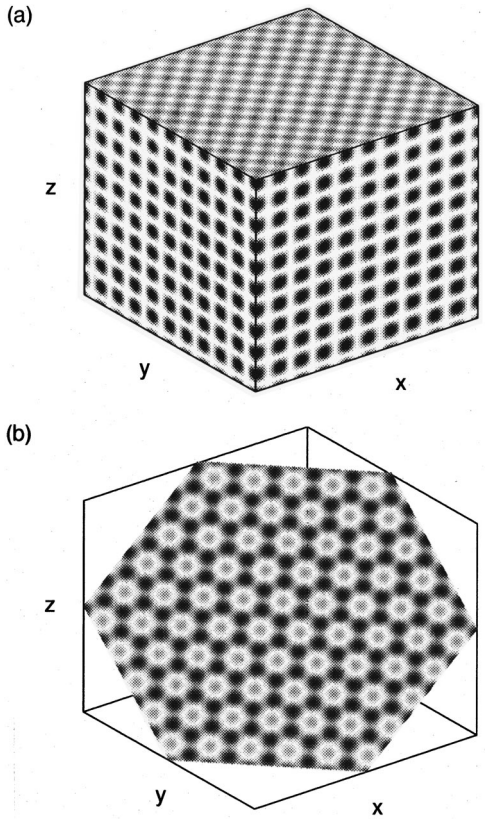


FIG. 2. A bcc pattern in the coordinates $(x,y,z)$. (a) shows three sections: constant $x$, $y$, and $z$, respectively, where square patterns are seen. (b) shows the section $z=x+y$, where black-eye patterns are seen.

$$\boldsymbol{k}_1=(1,\sqrt{3},0),\quad \boldsymbol{k}_2=(2,0,0),\quad \boldsymbol{k}_3=\left(1,\frac{\sqrt{3}}{3},-\frac{2\sqrt{2}}{\sqrt{3}}\right). \tag{2.14}$$

Using the new coordinates, a projection of $\mathcal{L}$ on the plane $(X,Y)$ is shown in Fig. 3. The sections

$$Z=\frac{N}{2\sqrt{6}}, \tag{2.15}$$

where $N$ is an integer, consist of hexagonal lattices, and there are no lattice points between two layers of consecutive $N$. Lattice points in the layer $Z=0$ form a hexagonal lattice with wavelength 1 in the plane $(X,Y)$, and lattice points in consecutive layers, $Z=\pm 1/2\sqrt{6}$, project together in the plane $(X,Y)$ as a hexagonal lattice with wavelength $1/\sqrt{3}$. The projected wavelengths are in the ratio $\sqrt{3}$. Now it is crucial to note that the three generators (2.12) have the same length when seen as three-dimensional vectors. This implies that the corresponding plane waves bifurcate together and possibly superimpose to provide the structure of the black-eye pattern.

### D. Comparison with the experiment

We call the space between two Secs. (2.15) with consecutive $N$ a *monolayer*. More formally, a monolayer is the three-dimensional slice

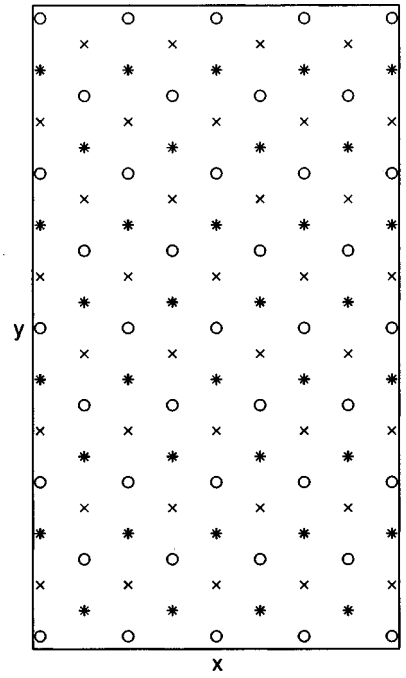


FIG. 3. Projection of a normalized bcc lattice on the plane $(X,Y)$. Sections of constant $Z$ are hexagonal lattices. Points marked with circles correspond to sections of the form $Z=3n/2\sqrt{3}$, points marked with crosses correspond to sections of the form $Z=(3n+1)/2\sqrt{3}$, and points marked with stars correspond to sections of the form $Z=(3n+2)/2\sqrt{3}$, where $n$ is an integer.

$$\mathcal{M}=\left\{(X,Y,Z)\in\mathbb{R}^3:\frac{N}{2\sqrt{6}}\leqslant Z\leqslant\frac{N+1}{2\sqrt{6}}\ \text{ for some }\ N\in\mathbb{Z}\right\}. \tag{2.16}$$

A monolayer of the bcc pattern in the coordinates $(X,Y,Z)$ is shown in Fig. 4(a). In experimental observations of chemical patterns, the optical resolution in the depth of the gel layer is not sufficient to separately resolve the pattern in each sec-

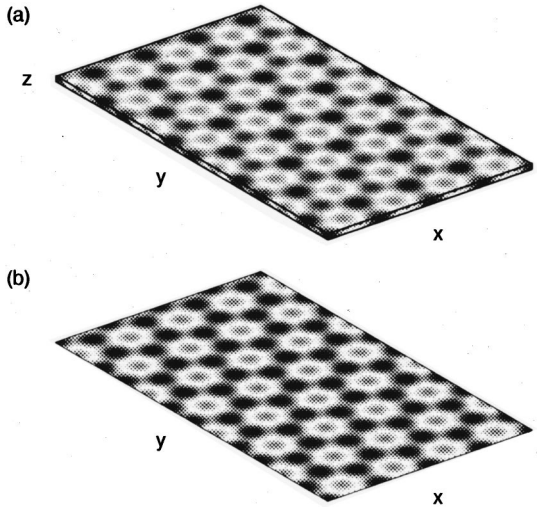


FIG. 4. A bcc pattern in the coordinates $(X,Y,Z)$ restricted to the monolayer $-1/4\sqrt{6}\leqslant Z\leqslant 1/4\sqrt{6}$. (a) shows the appearance of the pattern on the top-plane $Z=1/4\sqrt{6}$ and on the sides. (b) shows the integral over the depth $1/2\sqrt{6}$ of the monolayer.

tion. The photograph in Fig. 1 represents the integral of the experimental pattern over the thickness of the gel layer. The integral of the bcc pattern in Fig. 4(a) over the monolayer depth shows up the black-eye pattern [see Fig. 4(b)].

## III. DISCUSSION

This paper establishes a correspondence between bcc and black-eye patterns. After a suitable change of coordinates we find a black-eye pattern in a monolayer of a bcc pattern, suggesting that the two patterns are the *same*. Mathematically, the correspondence is established here. Physically, whether the proposed scenario corresponds to what happens in the experiments of Ouyang and Swinney is a challenging problem that deserves to be carefully discussed and further investigated. This discussion intends to clarify some issues related to the applicability of this theory, contribute to an ongoing debate about the dimensionality of chemical patterns in thin domains, and propose further investigations on three fronts: experiments, mathematics, and computations.

### A. Hidden symmetries

Naively, one would not expect a small aspect ratio system to exhibit any symmetries that do not leave the domain invariant. However, when only the symmetries of the domain are taken into account, it is not unusual to find unexpected conjugacies and unexpected highly developed patterns. Often the boundary conditions allow the system to inherit some of the Euclidean symmetries of the model partial differential equations (PDEs). These spatial symmetries are called *hidden symmetries*. Of particular interest are the translational hidden symmetries in multidimensional rectangles theoretically addressed by Gomes and Stewart [22], and carefully tested on the Faraday experiment by Crawford *et al.* [23]. Rotational hidden symmetries have also been detected and investigated. Theoretical results were applied to a variety of systems, including reaction-diffusion, convection, solidification of binary fluids, Kuramoto-Sivashinsky, Faraday experiment, elastic buckling (see the review article [14]).

In very broad terms, hidden symmetries are uncovered by extending the problem periodically to a larger one without boundaries, and then restricting to the subspace containing the solutions that satisfy the original boundary conditions. Whether or not such an extension can be made depends on the model PDE, the shape of the domain, and the boundary conditions.

To place the present paper in perspective, we should say that it uncovers spatial hidden symmetries in the CIMA reaction experiments of Ouyang and Swinney. Previous results on hidden symmetries and their successful application to physical and numerical experiments were certainly a key motivation for the approach presented here. The technique described in Sec. II can be developed into a variant of standard hidden symmetry methods, which should lead to more detailed predictions. Modifications of the standard methods are needed to accommodate features present in the CIMA reaction experiments. In particular, the thickness of the ''patterned layer'' and the conditions imposed by its ''boundaries'' are delicate issues deserving careful investigation on experiments, mathematics, and computations.

### B. Euclidean symmetries in the CIMA reaction

It is well accepted in the literature that reaction-diffusion systems are modeled by E(3)-invariant systems of coupled PDEs together with more or less appropriate boundary conditions (see, for example, Refs. [12] and [13]). Consequently, any potential deviation from $E(3)$ symmetry should originate in conditions imposed by the domain boundaries. In the particular case of Ouyang and Swinney's experiments, we do not expect boundary effects to be significant enough to change the nature of the intrinsic Turing patterns. More concretely, if in the absence of boundaries the most stable three-dimensional pattern has bcc symmetry (as predicted in Ref. [11]) the boundaries may have a perturbing effect, but it is very unlikely that they will lead to the selection of a two-dimensional pattern instead, no matter how thin the domain may be. This belief is substantiated by the comparison of two sets of experiments. For ease of exposition, the cartesian coordinates $X,Y,Z$ are introduced.

1. A set of experiments on the CIMA reaction was performed in Bordeaux as reported in Ref. [8]. The reaction occurred in a rectangular layer of gel with dimensions in milimeters $(L_X,L_Y,L_Z)=(20,3,1)$. The reactants were fed through the planes $Y=0,3$, producing a chemical gradient in the $Y$ direction. Visualizing the directions $X,Y$, the authors observed the formation of patterns in the central region of the reactor. In particular, a regular array of spots was observed. The reported wavelength of this structure was approximately 0.2 mm. The observations led the authors to speculate that (a) the patterns are three-dimensional because the wavelength is smaller than any geometric size of the reactor; (b) in the region where patterns can be observed, the spot distribution is in qualitative agreement with a three-dimensional bcc structure. This experimental result motivated further mathematical and computational work on bifurcations with bcc symmetry (see, for example, Refs. [12] and [13]).

2. In Austin, the CIMA reaction experiments (as described in Ref. [6]) were performed in a circular layer of gel with a diameter of 25 mm in the plane $(X,Y)$ and a thickness of 1 mm in $Z$. The reactants were fed through the planes $Z=0,1$, producing a chemical gradient in the $Z$ direction. The visualized directions were $X,Y$, and a sequence of patterns formed as a control parameter was varied. In particular, a hexagonal array of white spots with wavelength approximately 0.15 mm formed, and further up in parameter value, smaller black spots appeared in the center of the white spots (black-eye pattern). All patterns formed in a layer that was much thinner than the gel thickness. The speculations made by the authors about the dimensionality of the observed patterns were as follows: (a) The thickness of the pattern is comparable to the wavelength, and hence the patterns are essentially two-dimensional. (b) The black-eye pattern is a spatial harmonic generated by nonlinear interactions of the basic modes responsible for the two-dimensional hexagonal pattern.

What is the reason for such different interpretations of the two experiments? If the Austin experiments were significantly anisotropic to select two-dimensional patterns only, then why does the same not apply to the Bordeaux experiments? The main difference is that in the Bordeaux experiments the chemical gradient is imposed in a direction where

the gel is 3 mm thick, while in the Austin experiments this gradient is imposed in the thinner direction of 1 mm of gel. However, the patterns are reported to form in a layer that is much thinner than the gel layer. The fraction of the domain that we are interested in is relatively far from the feeding boundaries in both cases, and therefore it would not seem unreasonable if the effect of boundary conditions on the selected patterns was no more than a distortion. Furthermore, concerning the Austin experiments, Qi Ouyang explained (in a recent private communication) that the gel was sandwiched with porous glass (0.4 mm thick), the diffusion of which is typically 5 times lower than that of gels. This brings the effective thickness of each glass layer close to 1 mm, further reducing the significance of boundary effects in the pattern selection.

A different question is: What happens at the ''boundaries'' of the ''patterned layer,'' and how does that constrain the pattern selection? Numerical investigations of this problem were made possible by the proposal of a realistic model of the simpler chlorite dioxide-iodine-malonic acid (CDIMA) reaction by Lengyel, Rabai, and Epstein (LRE) [24]. Using this model, Setayeshgar and Cross [25] analyze numerically the one-dimensional patterns formed along the gradients imposed by boundary feeds and study their linear stability to symmetry-breaking perturbations in a direction transverse to these gradients. In Sec. VI of Ref. [25] the authors suggest further investigations that, amongst other things, should help to answer the question posed at the beginning of this paragraph. It should be very interesting to see how such investigations support our proposal that the described CIMA reaction experiments reveal approximate $E(3)$ symmetry in the ''patterned layer.''

### C. Bifurcation sequence

In our theoretical setup, the wavelength of the pattern and the thickness of the monolayer are in the ratio $2\sqrt{6}:1$. Whether the bcc symmetry is exact or only approximate depends on arguments that involve the above ratio and the boundary conditions on both sides of the patterned layer. Bifurcation to the bcc (or black-eye) pattern occurs directly from the uniform state in problems exhibiting exact bcc symmetry [13,17,20]. We expect the same pattern to occur as a higher branch in bifurcation problems where the bcc symmetry is only approximate. In the experiments of Ouyang and Swinney, black-eye patterns were observed as a secondary bifurcation (see the bifurcation sequence in Ref. [6]) and the ratio of the pattern wavelength and monolayer thickness is comparable to the value associated with our theoretical monolayer. The deduction of bifurcation diagrams with approximate bcc symmetry, and the planform visualization in the appropriate coordinates are points needing further investigation. The mathematical setting introduced in Sec. II is a starting point for further work using standard methods of symmetric bifurcation theory [2].

The results of the mathematical investigation proposed in the above paragraph should be closely compared with controlled experiments on the CIMA reaction. For that it is important to obtain a good understanding of how the pattern selection in the experiment varies with the thickness of the gel layer.

## IV. CONCLUSIONS

Including the third dimension may lead very naturally to bifurcations to black-eye patterns in thin domains. In the scenario introduced here, the black-eye pattern is a linear mode. We propose this technique as a method by which to uncover spatial symmetries that are not expected in two dimensions. Together with all the present uncertainties associated with the ''boundaries'' of the ''patterned layer'' in the experimental setting and the difficulties in resolving its thickness, we argue that the observations are well within our scenario for a bifurcation with approximate bcc symmetry. There are other nonstandard patterns whose relations with theoretical studies performed in two or three dimensions are still being debated (see, for example, Ref. [26]). The technique introduced in this paper is very general and it may be applicable to other situations.

Finally, the black-eye pattern is of interest in other fields of science, in particular morphogenesis (see, for example, Ref. [27]). There is evidence of black-eye patterns in animal coats, and the mechanism underlying its selection is not at all understood. Numerical simulations of reaction-diffusion models in two dimensions reproduce several of the experimentally observed Turing patterns, but they fail to reproduce the black-eye pattern (see Table 1 of Ref. [27]). We express here a strong conviction that black-eye patterns can be produced by three-dimensional simulations in thin domains. Such simulations should provide important information to a clarification of essential issues concerning the pattern thickness and its boundaries.

## ACKNOWLEDGMENTS

The author thanks Patrick De Kepper, Ana Dias, Ute Ebert, Marty Golubitsky, Greg King, Isabel Labouriau, Qi Ouyang, Ian Stewart, and Harry Swinney for helpful discussions. This research was initiated during a visit to the Institute for Mathematics and Its Applications, University of Minnesota. Both the IMA and program PRAXIS XXI of the Portuguese Fundação para a Ciência e Tecnologia contributed financial support.

[1] J. D. Murray, J. Theor. Biol. **88**, 161 (1981); Sci. Am. **258**, 80 (1988); *Mathematical Biology*, Vol. 88 of *Biomathematics Text Books*, edited by S. A. Levin (Springer-Verlag, New York, 1989).

[2] M. Golubitsky, I. N. Stewart, and D. Schaeffer, *Singularities and Groups in Bifurcation Theory Vol. 2*, Applied Mathematical Sciences Vol. 69 (Springer-Verlag, New York, 1988).

[3] M. Golubitsky, J. W. Swift, and E. Knobloch, Physica D **10**, 249 (1984).

[4] A. C. Newell and J. A. Whitehead, J. Fluid Mech. **38**, 279 (1969); L. A. Segel, *ibid.* **38**, 203 (1969).

[5] G. H. Gunaratne, Phys. Rev. Lett. **71**, 1367 (1993).

[6] G. H. Gunaratne, Q. Ouyang, and H. L. Swinney, Phys. Rev. E **50**, 2802 (1994).

[7] A. Turing, Philos. Trans. R. Soc. London, Ser. B **237**, 37 (1952).

[8] V. Castets, E. Dulos, J. Boissonade, and P. De Kepper, Phys. Rev. Lett. **64**, 2953 (1990); P. De Kepper, V. Castets, E. Dulos, and J. Boissonade, Physica D **49**, 161 (1991).
[9] Q. Ouyang and H. L. Swinney, Nature (London) **352**, 610 (1991); Chaos **1**, 411 (1991); in *Chemical Waves and Patterns*, edited by R. Kapral and K. Showalter (Kluwer, Dordrecht, 1994).
[10] S. Alexander and J. McTague, Phys. Rev. Lett. **41**, 702 (1978).
[11] D. Walgraef, G. Dewel, and P. Borckmans, Adv. Chem. Phys. **49**, 311 (1982).
[12] A. De Wit, G. Dewel, P. Borckmans, and D. Walgraef, Physica D **61**, 289 (1992); A. De Wit, P. Borckmans, and G. Dewel, Proc. Natl. Acad. Sci. USA **94**, 12 765 (1997).
[13] T. K. Callahan and E. Knobloch, Physica D **132**, 339 (1999).
[14] M. G. M. Gomes, I. S. Labouriau, and E. M. Pinho, in *Pattern Formation in Continuous and Coupled Systems*, edited by M. Golubitsky, D. Luss, and S. Strogatz, IMA Volumes in Mathematics and its Applications (Springer-Verlag, New York, 1999).
[15] A. T. Winfree, *The Geometry of Biological Time*, Springer Study Edition (Springer-Verlag, Berlin, 1990).
[16] B. Dionne and M. Golubitsky, Z. Angew. Math. Phys. **43**, 36 (1992).
[17] B. Dionne, Z. Angew. Math. Phys. **44**, 673 (1993).
[18] W. Miller, *Symmetry Groups and Their Applications* (Academic Press, New York, 1972).
[19] C. Kittel, *Introduction to Solid State Physics* (John Wiley & Sons, Inc., New York, 1976).
[20] T. K. Callahan and E. Knobloch, Nonlinearity **10**, 1179 (1997).
[21] M. G. M. Gomes and I. Stewart, Int. J. Bifurcation Chaos Appl. Sci. Eng. **7**, 147 (1997).
[22] M. G. M. Gomes and I. Stewart, Nonlinearity **7**, 253 (1994).
[23] J. D. Crawford, J. P. Gollub, and D. Lane, Nonlinearity **6**, 119 (1993).
[24] I. Lengyel, G. Rabai, and I. R. Epstein, J. Am. Chem. Soc. **112**, 4606 (1990); **112**, 9104 (1990).
[25] S. Setayeshgar and M. C. Cross, Phys. Rev. E **58**, 4485 (1998).
[26] B. Rudovics, E. Dulos, and P. De Kepper, Phys. Scr. **T67**, 43 (1996); E. Dulos, P. Davies, B. Rudovics, and P. De Kepper, Physica D **98**, 53 (1996).
[27] P. K. Maini, K. J. Painter, and H. N. P. Chau, J. Chem. Soc., Faraday Trans. **93**, 3601 (1997).